INVESTIGATION OF GASDYNAMICS OF A MODEL WITH COMBUSTION IN A SHOCK TUNNEL

V. K. Baev, V. V. Shumskii, and M. I. Yaroslavtsev

UDC 536.46; 621.45.022

Experimental investigations in supersonic or hypersonic air streams in facilities modeling combustion processes are quite complex. There are difficulties with the large flow rates of high-enthalpy air, the complexity of the models with combustion and the technology of testing them at high temperatures, and with the fact that in the experiments one cannot fully model the working process and the force characteristics [1-4].

To overcome these difficulties one is led to the idea of using high-enthalpy facilities with a short-duration test regime for experimental study of processes in models with a heat supply. One of the first attempts to use short-duration facilities for these purposes is the shock tube investigations described in [5]. In spite of the very short useful experimental time (~3 msec), the authors of [5] were able to measure a number of flow parameters in the circuit of a gasdynamic model with combustion and even to elucidate the results obtained numerically (by means of a theoretical analysis). However, one should recognize that a test time of ~3 msec is not enough to investigate the operating process and particularly not enough for force characteristics, although the time to establish the boundary layer and separated zones on model surfaces is several milliseconds [6], and the variation in the nature of the flow within a model, associated with gasdynamic and thermodynamic phenomena, may occupy tens of milliseconds [7].

Another type of short-duration facility is the shock tunnel, a facility with a test time of from several hundredths to several tenths of a second [8]. Shock tunnels have been used for successful investigations of air compression in air intake devices, and for injection, mixing, and autoignition of fuels in an air stream [6, 9]. The results of these investigations have shown that shock tunnels can provide an entirely appropriate test facility for models with combustion in a high-enthalpy air stream.

In this paper we give results of investigations in the IT-301 shock tunnel [8] of the working process and force characteristics occurring in a gasdynamic model with internal ignition of hydrogen. The objectives of the model test were:

to obtain the model force characteristics;

to compare the experimental data with theory;

for the results of weighted measurements to evaluate the completeness of hydrogen combustion within the model;

to investigate the influence of operation of the internal circuit on the operation of the air intake model.

Results relating to comparison of theory and experimental values of force characteristics and pressure inside the model and relating to evaluation of the completeness of combustion from the weighted measurements have been presented in [7], and the present paper contains results relating to analysis of the working process from weighted data and drainage measurements and to the influence of operation of the internal circuit of operation of the air intake.

Figure 1 shows the layout of the model in the working section of the shock tunnel. A detailed description of the model and its test conditions have been given in [7]. Therefore we note only the range of parameters of the stream incident on the model on which measurements were taken during operation of the tunnel: the stagnation pressure and temperature $p_{oi}(\tau) = 70\text{-}7$ MPa/m^2, $T_{oi}(\tau) = 2250\text{-}1000$ °K, the static pressure and temperature $p_i(\tau) = 110\text{-}$

Novosibirsk. Translated from Zhurnal Prikladnoi Mekhaniki i Tekhnicheskoi Fiziki, No. 6, pp. 58-66, November-December, 1983. Original article submitted October 11, 1982.

 0021-8944/83/2406-0816$07.50

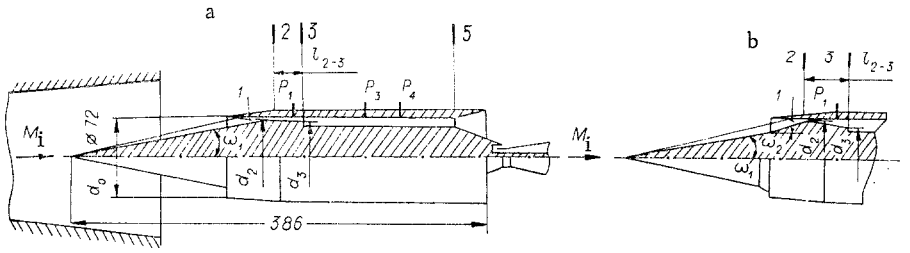

Fig. 1

20 GPa, $T_i(\tau)$ = 220-90°K, the Mach number M_i = 7.33, the velocity head $q_i(\tau)$ = 0.35-0.035 MPa, and the air flow rate through the model m_a = 1.4-0.25 kg/sec. Here τ = 0-55 msec is the ambient flow time, and the time origin was taken at the time of discharge of a capacitor bank in the driver chamber. The variation of incident air parameters during the test (values typical of shock tunnels and those for the present tests are: driver volume 1.14 dm^3; nozzle throat diameter 10 mm; discharge voltage of capacitor bank U = 4-5 kV) have been given, e.g., in [9].

Figure 1 shows the air intake configurations tested in making up the model: a) variant 1; b) variants 2 and 3. The use of air intakes in the form of simple cones is explained by the fact that in the shock tunnel a wave mechanism is achieved for starting the channel [10]. Therefore, in the shock tunnel the diffusers start up with a large geometric compression [6]. It has been shown in [11] that, the less is the relative area of the throat $f_2 = F_2/F_0$, the higher are the force characteristics of the internal channel. Here F_2 is the transverse cross-sectional area of the air intake throat (Sec. 2), $F_0 = \pi d_0^2/4$ is the area of the air intake entrance. Therefore in the tests f_2 was varied (see Table 1).

Air intake variant 1 with f_2 = 0.16 was started up at the beginning of the shock tunnel regime and remained flowing up to ~16 msec. The Reynolds number Re, based on the incident stream parameters and the length of the cone generator 0.19 m from the nose to the corner point, was $3.5 \cdot 10^6$ at the moment of flow separation. In order to increase the air intake operating time in the flow-on state the throat was increased from f_2 = 0.16 to f_2 = 0.18. Here the configuration of the throat remained in the form of a coaxial cylinder with $d_2 = d_3$. The air intake variant 1 with f_2 = 0.18 operated in the flow-on state for 37 msec. At the moment of flow separation we had $Re = 1.8 \cdot 10^6$. After the throat was increased to f_2 = 0.19 the air intake remained in the flow-on state throughout the entire shock tunnel regime, and flow separation set in only when the shocks from the nozzle rim reached the leading edge of the model support plate and broke down the flow regime in the model. At the time of flow breakdown we had $Re = 1.5 \cdot 10^6$.

In order to reduce f_2 (without using methods of reducing f_2 by varying the geometry of the support plate) we examined an air intake with a centerbody in the form of two cones, the variant 2 model. Flow separation occurred at 27 msec in the variant 2 air intake with f_2 = 0.16. Enlarging the throat to f_2 = 0.18 ensured operation of the variant 2 air intake in the flow-on state during the whole shock tunnel regime. We note that for variant 1 a throat with f_2 = 0.18 still did not ensure normal operation of the air intake for the whole shock tunnel regime.

Analysis of shadowgraph pictures of flow over the air intake, of the Reynolds number for which flow separation occurs in the air intake, of the measured pressure in the model channel and the results of a two-dimensional flow calculation have shown that two factors affect the flow-on duration of air intake variants 1-3 (depending on f_2 in the range f_2 = 0.16-0.19).

The first factor is the location of the shock reflected from the support plate relative to the air intake corner point. Calculation of the axisymmetric flow with adiabatic index 1.4 without allowing for the boundary layer on the centerbody and for a plane-parallel incident stream with M_i = 7.33 has shown that for air intake variant 1 with $f_2 \geq 0.19$ the shock 1 (see Fig. 1) reflected from the support plate falls on the corner point or behind it. The angle at which the shock meets the cylindrical surface of the throat of the air intake is small. Therefore, either the boundary layer will not separate, or the separated zone will be small. When f_2 is reduced from $f_2 \approx 0.19$ the corner point is moved downstream relative to the leading edge of the support plate, and the shock reflected from the support plate

TABLE 1

Air intake, variant and model	ω_1	ω_2	f_2	d_2, mm	d_3, mm	l_{2-3}, mm
1	10°		0,16	66	66	24
			0,18	65,2	65,2	26,5
			0,19	64,8	63,7	27,6
2	10°	19°	0,16	66	59	47
		16°	0,18	65,2	59	43
3	10°	15°42′	0,19	64,8	63,5	39

will fall even on the conical surface ahead of the corner point. Here the angle at which the shock meets the surface of the centerbody increases sharply: by $\omega_1 = 10°$ for air intake variant 1, and by $\omega_2 = 19°$-15°42′ for variants 2-3. Here the pressure drop when the two-shock system passes is ∿8.5 at a Mach number ahead of the corner point of $M \approx 5.7$. The boundary layer with transition or turbulent flow conditions cannot sustain the force acting on it, associated with a pressure increase of more than 4-7 at M = 5-6 without separating [12]. Therefore the presence of a pressure increase of a factor of 8.5 causes boundary layer separation on the conical surface ahead of the corner point for the air intake variant 1 with $f_2 < 0.19$. With increase of f_2 the distance increases from the point of shock incidence to the corner point. It was shown in [13] that when the shock falls ahead of the corner point the distance from the location of shock incidence to the corner point is important in generating flow separation in the air intake. With increase of this distance there is an increase of the mass of gas entering the separated zone. When it passes into the air intake throat the separation reduces the effective throat area the more, the greater is the mass of gas in the separation zone.

For air intake variants 2 and 3 the corner is displaced upstream because of the steeper second cone. Therefore the shock reflected from the support plate falls on the corner point at a smaller relative throat area, for $f_2 \approx 0.18$, than for variant 1.

It is interesting to note that boundary layer separation shows up (on the shadowgraph pictures of the flow) for all f_2 on the external compression surfaces of the air intake. Here the less is f_2, the greater is the part of the centerbody on which there is separation. For $f_2 = 0.16$ the separation leads to a rapid flow breakdown, and for $f_2 = 0.18$ for variant 1 the air intakes operate in the flow-on state in the presence of boundary layer separation on the external compression surface throughout the whole time of operation of the shock tunnel.

The second factor influencing the duration of the air intake in the flow-on state is a decrease of Re during the shock tunnel operation. The start-up of air intake variants 1-3 occurs at the start of operation of the tunnel, when $Re = (4.2 - 6) \cdot 10^6$. For these values of Re the boundary layer in the corner point region for $M \approx 5.7$ is in the turbulent or transitional flow regime. But with an increase of Re there is an increase of the length of the separated zone [14] ahead of the corner point for a boundary layer with a transition flow regime.

Thus, the two factors are evidence that flow separation in air intake variant 1 for $f_2 < 0.19$ and in intakes variants 2 and 3 for $f_2 < 0.18$ are associated with an increase of separation of the boundary layer on the centerbody at the location where the shock reflected from the support plate strikes. Here the boundary layer in the corner point region is in the turbulent or transitional flow regime during the whole tunnel operation, and is not laminar, since flow breakdown in air intake variant 1 with $f_2 = 0.19$ and in variants 2 and 3 with $f_2 = 0.18$ occurs due to cessation of tunnel operation and not because of reduction of Re to a value for which the boundary layer would become laminar in the corner point region.

The tests with combustion of gaseous hydrogen in the model were conducted in the range of excess air coefficients $\alpha = 1.6$-3 for $\alpha \approx$ const during each test.

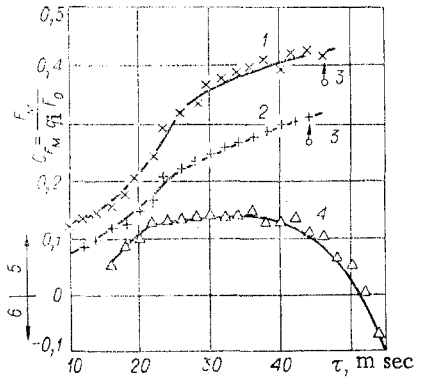

Fig. 2

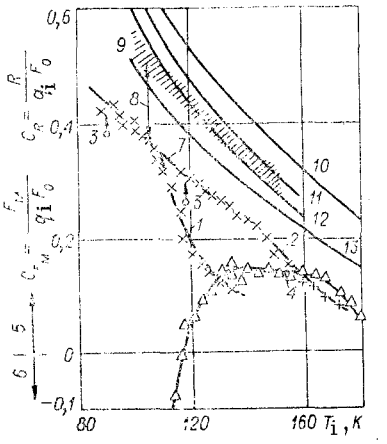

Fig. 3

It was shown in [7] that the time required to reform the flow (caused by heat input from combustion of hydrogen in autoignition conditions) in the model from the supersonic regime established in the first 2 msec of tunnel operation to subsonic is 20-28 msec. Thereafter the model combustion chamber (sections 2-5 of the model circuit, see Fig. 1) operates with combustion of hydrogen in subsonic flow or up to the end of operation of the tunnel, or until flow separation of the air in the model. Thus, beyond the time of operation of the tunnel with variable test conditions there is a change in the model operating regime: for a regime of heat supply to a supersonic flow in a chamber combustion chamber to a regime of heat supply to a subsonic flow in the combustion chamber.

Figure 2 [which shows the thrust (or drag) coefficient C_{F_M} of the model as a function of time, with combustion of hydrogen in the model with α = 1.6-1.7] indicates two typical tests: in one test, which we call curve 1, the heat supply regime ends at 26 msec, and at 24 msec in the test relating to curve 2 (3 is air flow separation in the model and cessation of combustion, 5 is the model thrust, and 6 is the model drag). Here F_M is the force applied to all the model surfaces and measured by means of a one-component aerodynamic balance.

However, in the tests with this model another situation arose where no quasistable state was observed at the end of the transition process (in terms of the thrust and the pressure inside the model), but only a certain band of C_{F_M} in the region of 24-40 msec, and then a drop in thrust. This situation only occurred with the maximum energy input to the tunnel driver, i.e., at high initial values T_{oi} of the incident air, which seems strange at first sight, since the higher is T_{oi} the better would appear to be the conditions for hydrogen combustion. One of these "unsuccessful" tests is shown in Fig. 2 (curve 4).

Figure 3 shows data on the thrust (or drag) coefficient C_{F_M} of the model for the three tests shown in Fig. 2, drawn as a function of the static temperature T_i of the incident stream (the symbols 1-6 are the same as in Fig. 2).

It can be seen by comparing curves 1, 2, and 4 in Figs. 2 and 3 that the rate of increase of C_{F_M} at the start of the regime before ~24 msec is the same for all three tests, i.e., before ~24 msec the increase of C_{F_M} as a function of T_i, and therefore, of the relative heating of the test body, is the same, where $\theta = T_{os}/T_{oi}$ is the stagnation temperature of the combustion products at the chamber exit. However, for the tests described by curves 1 and 2, at τ = 24-26 msec there was a change of the heat supply regime, and after τ = 24-26 msec the combustion of hydrogen in these tests occurred on the average for a subsonic gas velocity in the chamber, i.e., for more favorable conditions for combustion than if the gas velocity in the combustion chamber remained supersonic.

For the tests described by curves 1 and 2 in Figs. 2 and 3 the temperature T_i was 110 and 147°K during the change of the heat supply regime (at τ = 26 and 24 msec, respectively). For the test described by curve 4, for τ = 24 msec, we have T_i = 167°K. In assuming the same completeness of combustion ξ for all three tests the value of θ for the test described by curve 4 should be less at τ = 24 msec by ~34% and by ~12% than at the time of shift of

the heat supply regime for the tests described by curves 1 and 2, respectively. While in the tests described by curves 1 and 2 at τ = 24-26 msec the shift of heat supply regime occurred, for the test described by curve 4 the relative heating of the working substance so that the change of heat supply regime would occur in the model should be increased by 10-30% compared with the value of θ which occurred in this test before 24 msec (for the same increase of C_{F_M} and with no change of the completeness of combustion this should occur for τ > 32 msec). But before 32 msec for the test described by curve 4 the quantities p_i and T_i decrease, compared with their values at the beginning of the operation, by a factor of 4.4 and 40%, respectively. The tests conducted have shown that if the change of heat supply regime has not occurred before 20-28 msec, then, because of the considerable decrease of pressure and temperature in the model circuit, the subsequent combustion of hydrogen in the supersonic stream will not achieve a sufficient completeness of combustion to increase θ to a value for which a change of heat supply regime would occur in the model: For τ > 20-28 msec the combustion of hydrogen in the supersonic stream in the model is gradually attenuated, although it is not stopped completely. Incidentally, evidence of the strong influence of pressure on the conditions for combustion of hydrogen in the model in the autoignition regime is the fact that on separation of the air flow into the intake device the combustion in the model immediately ceases, since the pressure in the model circuit falls sharply by a factor of ~4 when the flow separated (see 3 in Figs. 2 and 3).

Thus, the condition for reaching, before 20-28 msec, a value of θ to ensure a change of the heat supply regime in the combustion chamber, given the conditions of the model test in the IT-301 shock tunnel, is a governing factor to obtain experimental information in the tests on the pressure distribution inside the circuit and the model force characteristics. In the tests with U > 4.6 kV, $T_{oi}(0)$ > 2000°K this condition is not always fulfilled. In [7] and in the present work only tests are considered for which one can say that a change in the heat supply regime occurred and for τ > 20-28 msec the heat was supplied to the subsonic stream.

After subsonic combustion was established in the model the data on the model thrust coefficient C_{F_M} obtained in experiments at various T_i, fall very well on a single curve (see Fig. 3, curve 7). This curve describes the thrust of model variant 1, the force applied to the entire model surface during combustion within it of hydrogen with α = 1.7 in the subsonic flow.

The internal thrust of the model R, i.e., the force applied only to the internal surface of the model circuit, is larger than the force measured by the balance F_M, by the drag of the support plate. The internal thrust characteristics are usually calculated under the approximation that there is no loss of heat in the chamber from hydrogen combustion. The calculations performed have shown that the model support plate drag coefficient, consisting of the wave drag and the friction drag, is 0.04-0.05, and that at the wall the model loses 10.5-15.5% of the heat released from hydrogen combustion.

If in Fig. 3 to the model thrust coefficient C_{F_M} measured by the balance (curve 7) we add the support plate drag coefficient and the thrust coefficient that would be created by the working substance due to the 10.5-15.5% of heat released in hydrogen combustion to the model walls (intercept 8), then region 9 gives the model internal thrust coefficient generated by the internal model circuit in the tests at the actual values of the coefficient of completeness of combustion. Thus, region 9 in Fig. 3 shows the experimental values of the internal thrust coefficient C_R of the variant 1 model obtained by introducing corrections to the model thrust coefficient C_{F_M} measured by the balance. Region 9 can be compared with theoretical values of the internal thrust coefficient.

Figure 3 shows theoretical values of $C_R = f(T_i)$ for the variant 1 model for two values of completeness of combustion: ξ = 0.9 (curves 10-12) and ξ = 0.7 (curve 13). There is some indeterminacy in comparing the experimental and theoretical values of C_R, associated with lack of knowledge of the level of loss in the model nozzle. We therefore made parametric calculations, varying the nozzle velocity coefficient φ_c and determining its influence on C_R. Figure 3 with ξ = 0.9 shows curves of C_R for φ_c = 0.98; 0.96, and 0.94 (curves 10-12, respectively).

It can be seen from Fig. 3 that, even taking the losses in the model nozzle as insignificant (on the order of 0.98), the completeness of combustion of hydrogen in the model

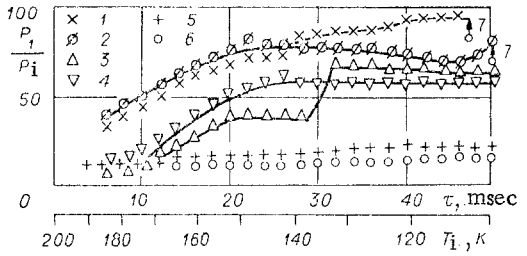

Fig. 4

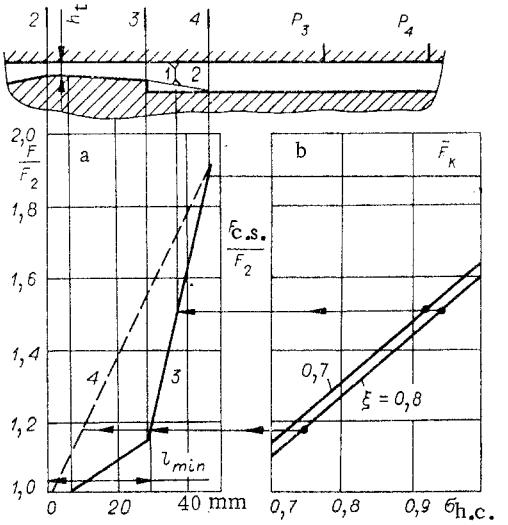

Fig. 5

corresponding to the experimental values of C_R, is quite high: for T_i = 140-150°K ξ lies in the range 0.8-0.9. With decrease of T_i the completeness of hydrogen combustion in the model decreases, although the experimental values of C_R in region 9 mainly follow the theoretical dependence $C_R = f(T_i)$: At T_i = 100°K the values of ξ lie in the range 0.7-0.8. This occurs because with decrease T_i (with increase of the regime time τ) there is a strong decrease of p_i: In a time of 50 msec p_i decreases by a factor of 10, and T_i by a factor of 1.8-2.0. But with a decrease of p_i and T_i there is a proportional decrease of the pressure and temperature in the model, i.e., a worsening of conditions for hydrogen ignition, leading to a decrease of the completeness of combustion for reduced values of T_i.

The boundary between the air intake device and the combustion chamber is assigned quite arbitrarily. In a number of cases, i.e., in investigating air intakes, it is convenient to take this boundary as section 3 [13]. In investigating the entire model with internal ignition of hot substance the nature of the flow in the model circuit and the presence or absence of transition from supersonic combustion to subsonic is determined by θ and the expansion of the combustion chamber $\bar{F}_C = F_3/F_2$, i.e., the flows in sections 2—3 and 3—5 are coupled and interdependent. Therefore, from the viewpoint of the function of the individual elements of the model and the viewpoint of creating a computational technique [15] it is convenient to assign section 2—3 to the combustion chamber. It is from this viewpoint that the part of the model circuit between sections 2—5 is considered as the combustion chamber in this paper. Then the influence of the combustion chamber on the operation of the air intake is considered to be as follows. If perturbations from the combustion chamber due to an increase of pressure in it are transmitted upstream beyond section 2 to the compression surfaces of the air intake, then the combustion chamber influences the operation of the air intake, since the transmission of perturbations to the compression surfaces leads, as a rule, to flow separation in the air intake. But if the perturbations from the combustion chamber are not transmitted through section 2 to the compression surfaces, then the operation of the combustion chamber does not influence that of the air intake.

Figure 4 shows the pressure, referenced to p_i, at the point p_1 located at section 2—3 of the combustion chamber: 1) α = 1.6-1.8; 2) α = 1.65-1.7; 3) α = 2.5; 4) α = 3; 5, 6) with no hydrogen supply to the model; 7) flow separation in the model and cessation of combustion). It can be seen that the greater is the combustion of hydrogen, the higher is the pressure in section 2—3. In the tests with pressure measurement at points p_1, p_3, p_4 of the model motion pictures were also taken of the flame through a window in the support. The movie picture results showed that the flame was not thrown forward to the initial section of the combustion chamber, but was located, beginning either at the shoulder, or from the point where the injectors were located (depending on α and the regime time), and the pressure increase at the section p_1 is not associated with the presence of hydrogen combustion at section 2—3, but with transition of the supersonic flow to subsonic in the initial section of the combustion chamber. In fact, the flow transition in the channel from supersonic to subsonic at M > 2 occurs in a pseudoshock [16, 17]. The pseudoshock has a thickness and spans the point p_1 where the pressure increase is observed. It follows from this that beyond the throat of the

air intake there must be a margin of length such that the origin of the pseudoshock is located at section 2—3 and does not move upstream against the flow above the corner point of the air intake.

In the calculations of force characteristics and parameters of the working substance in the model circuit one usually does not have a pseudoshock but a normal shock [15], assuming that the calculated parameters of the subsonic flow behind the normal shock agree very well with the parameters behind the pseudoshock [16]. It is therefore of interest to evaluate the location in the combustion chamber where the normal shock should be located immediately before the time of flow separation in the model.

The theoretical location of the normal shock can be determined, starting with the values of T_i and T_{oi} and the measured pressure in the combustion chamber at the time of flow separation in the model. The separation of the flow into the model for $\alpha \approx 1.7$ in the different tests occurred at different tunnel operating times, but in rather a narrow range of T_i (on the average for $T_i \approx 108°K$). Here the degree of pressure increase in the model combustion chamber at the points p_3 and p_4 was $p_3/p_i \approx p_4/p_i \approx 125$. Since we do not know the hydraulic losses in the combustion chamber accurately, we made parametric calculations to determine the location of the normal shock 2 (Fig. 5) for $\sigma_{h.c.} = 0.7$-1. Here $\sigma_{h.c.}$ is the total pressure recovery factor corresponding to the hydraulic losses in the chamber; the hydraulic losses include all types of total pressure loss, besides the loss in the normal shock and the thermodynamic losses associated with the supply of heat: losses to friction; to flow over the shoulder; the pylons; the injectors; etc. [7].

On the basis of these data we calculated the cross sections of the combustion chamber $F_{c.s.}/F_2 = f(\xi, \sigma_{h.c.})$, at which the normal shock was located (Fig. 5b), and here $F_{c.s.}$ is the cross-sectional area of the combustion chamber where the normal shock is located. Since $\xi = 0.7$-0.8 at the end of the regime, the calculations were performed for $\xi = 0.7$ and 0.8. Figure 5a shows the variation of cross-sectional area (curve 3) along the combustion chamber. Here it was assumed that the expansion of the chamber behind the shoulder occurred along the dividing streamline 1, and that the length of the stagnation zone was 6 shoulder heights [18]. Estimates made using the drag coefficients taken from [19] have shown that in the segment from section 2 to the end of the combustion chamber the total pressure losses associated with hydraulic losses do not exceed 0.25-0.2, i.e., $\sigma_{h.c.} > 0.75$-0.8 (with subsonic heat supply). Therefore, it follows from Fig. 5 that the normal shock that the values considered $\xi = 0.7$-0.8 and $\sigma_{h.c.} > 0.75$ will be located in the stagnation zone behind the shoulder.

For the very unfavorable set of quantities $\sigma_{h.c.} = 0.75$ and $\xi = 0.8$ for the variant 1 model the value $F_{c.s.}/F_2 \approx 1.2$, and the distance from the air intake throat to the normal shock location is $l_{min} = 28$ mm. Here l_{min} is the minimum distance from the throat to the normal shock, the least value that one can establish for the distance between section 2 and the theoretical shock in the thermodynamic calculation. If for some model operating regime the distance between section 2 and the calculated value of the normal shock is less than l_{min} (in fact this means that the origin of the pseudoshock is above the air intake throat), then in the operation of the model there must be separation of the flow into the air intake. On the other hand, if in the model operation the distance between section 2 and the calculated value of the normal shock is greater than l_{min} (in fact this means that the origin of the pseudoshock will be either in the air intake throat, or downstream of the throat), then the operation of the combustion chamber will not influence the air intake operation.

From Fig. 5 one can conclude (since one is considering the time immediately ahead of separation of air flow to the model) that the flow separation for $T_i \leq 108°K$ (for $\alpha = 1.7$, $\xi = 0.7$-0.8) does not occur because of thermal cutoff of the combustion chamber, since there is still at least 20% margin of area, but because the place where the pressure increase in the combustion chamber due to flow transition from supersonic to subsonic is located too close to the air intake throat.

According to the work of [16], the length of the pseudoshock for the values M = 4.5-5.3 which we had in the present model behind the air intake throat and ahead of the pseudoshock, is 12-15 calibers if one does not have the phenomenon called pseudoshock fixation in [17], and therefore the relative distance l_{min}/h_t 8, where h_t is the height of the air intake throat, comparable with the length of the pseudoshock, although somewhat less than the length of the pseudoshock.

With the help of the above reasoning one can explain why in model variant 2 ($f_2 = 0.18$) we observe separation of the air flow into the model immediately after the hydrogen is supplied to it. Curve 4 of Fig. 5a shows the relative cross-sectional area of the combustion chamber behind the air intake throat for the variant 2 model with $f_2 = 0.18$. It can be seen that for these values of $\sigma_{h.c.}$ and ξ in the variant 2 model the location of the strong pressure increase (in the calculated normal shock model) will be considerably closer to the air intake throat than in variant 1. Thus, for $\sigma_{h.c.} = 0.75$ and $\xi = 0.8$ the shock for the variant 1 model will be located at a distance $l_{min}/h_t \approx 8$ from the throat, but for variant 2 at a distance less by a factor of 2.5, i.e., for the variant 2 model the origin of the pseudoshock must be located above the air intake throat, which leads to the immediate separation of flow to the model. By taking a single step — displacing the location of the strong pressure increase farther from the air intake nozzle (going from the variant 2 to the variant 3 model, which differs from variant 2 only in having less expansion of the centerbody in section 2—3, because of which the location of the strong pressure increase is even somewhat less distant, by length l_{2-3}, from the air intake throat than in variant 2) one can ensure hydrogen combustion in the model for the same air intake configuration. A sudden displacement of the pseudoshock upstream against the flow was observed in [17]. As analogous phenomenon was observed also in tests with the present model. For instance, Fig. 4 shows a test with $\alpha = 2.5$ in which the pressure at the point p_1 showed no significant increase prior to $\tau = 30$ msec, but at $\tau \geq 30$ msec a stepwise pressure increase occurred. And here the pressure at points p_3 and p_4 remained practically unchanged. Figure 4 also shows two tests with $\alpha \approx 1.7$ (1 and 2) for which the pressure at point p_1 is different, beginning at $\tau \approx 30$ msec and continuing up to flow separation into the model, although the pressures at the points p_3 and p_4 coincide very well in these tests. All of this is evidence that the phenomenon of flow transition in the initial section of the combustion chamber from supersonic to subsonic is to some extent unsteady, and is not rigorously associated only with the thermodynamic and the geometry of the combustion chamber.

LITERATURE CITED

1. R. I. Kurziner, Jet Engines for High Supersonic Flight Velocities [in Russian], Mashinostroenie, Moscow (1977).
2. V. S. Zuev and V. S. Makaron, Theory of Single-Pass and Rocket Single-Pass Engines [in Russian], Mashinostroenie, Moscow (1971).
3. S. M. Shlyakhtenko (ed.), Theory of Air Jet Engines [in Russian], Mashinostroenie, Moscow (1975).
4. V. K. Baev, V. A. Konstantinovskii, and P. K. Tret'yakov, "Modeling of the GPVRD combustion chamber," in: Gasdynamics of Combustion in Supersonic Flow [in Russian], Novosibirsk (1979).
5. Y. T. Osgerby, H. K. Smithson, and D. A. Wagner, "Supersonic combustion tests with a double-oblique-shock Scramjet in a shock tunnel," AIAA Paper N 827 (1969).
6. B. V. Boshenyatov, B. N. Gilyazetdinov, and V. V. Zatoloka, "Experimental investigations of hypersonic air intakes," in: Aeromechanics [in Russian], Nauka, Moscow (1976).
7. V. K. Baev, V. V. Shumskii, and M. M. Proslavtsev, "Investigation of the operation of a dual-regime combustion chamber with a subsonic heat supply regime," in: Gasdynamics of Flow in Nozzles and Diffusers [in Russian], Novosibirsk (1982).
8. A. S. Korolev, B. V. Boshenyatov, I. G. Druker, and V. V. Zatoloka, Shock Tunnels in Aerodynamic Research [in Russian], Nauka, Novosibirsk (1978).
9. V. K. Baev, B. V. Boshenyatov, Yu. A. Pronin, and V. V. Shumskii, "Experimental investigation of ignition of hydrogen injected into a supersonic stream of heated air," in: Gasdynamics of Combustion in a Supersonic Stream [in Russian], Novosibirsk (1979); "Investigation of liquid injection into a supersonic stream of high-enthalpy gas," Fiz. Goreniya Vzryva, 17, 3 (1981).
10. A. I. Lashkov and A. A. Nikol'skii, "Wave-actuated start-up of a supersonic diffuser," Inzh.-Zh., 2, 1 (1962).
11. V. V. Zatoloka, V. I. Zvegintsev, and V. V. Shumskii, "The influence of the compression process in an air intake on the specific thrust characteristics of GPVRD," Izv. Sib. Otd. Akad Nauk SSSR, No. 8, Ser. Tekh. Nauk No. 2 (1978).
12. M. A. Gol'dfel'd and V. N. Dolgov, "Development of a turbulent boundary layer after interaction with a density discontinuity," Izv. Sib. Otd. Akad. Nauk SSSR, No. 13, Ser. Tekh. Nauk No. 3 (1976).

13. V. G. Gurylev and E. V. Piotrovich, "Flow separation at the entrance to a supersonic air intake," Uch. Zap. Tsentr. Aero. Gidro. Inst., 5, No. 3 (1974).
14. M. A. Gol'dfel'd, V. V. Zatoloka, and É. G. Tyutina, "Experimental investigation of the separation properties of a boundary layer ahead of a rectangular obstacle in a cylindrical tube," Izv. Sib. Otd. Akad. Nauk SSSR, No. 8, Ser. Tekh. Nauk. No. 2 (1975).
15. Yu. A. Saren and V. V. Shumskii, "Characteristics of a GPVRD with a two-regime combustion chamber," in: Gasdynamics of Flows in Nozzles and Diffusers [in Russian], Novosibirsk (1982).
16. G. Emmons (ed.), Fundamentals of Gasdynamics [Russian translation], IL, Moscow (1963).
17. V. G. Gurylev and A. K. Trifonov, "A pseudoshock in a very simple air intake in the form of a cylindrical tube," Uch. Zap. Tsentr. Aero. Gidro. Inst., 7, No. 1 (1976).
18. P. K. Chang, Separation of Flow, Pergamon (1970).
19. I. E. Idel'chik, Hydraulic Drag Handbook [in Russian], Gosénergoizdat, Moscow–Leningrad (1960).

EXISTENCE OF SOLUTIONS FOR THE SYSTEM OF EQUATIONS DESCRIBING THE FILTRATION OF A BURNING GAS

Yu. M. Laevskii

UDC 536.46

A two-temperature model describing the propagation of combustion waves in a chemically inert porous medium was discussed in [1] for the filtration of a combustible gas mixture. The approximate solution obtained there described satisfactorily the experimental results obtained at the Institute of Chemical Kinetics and Combustion (Siberian Branch, Academy of Sciences of the USSR). The physical basis of the process is the recovery of energy from conductive transport in the solid structure and heat exchange between the phases. Pressure gradients are ignored in the treatment; this corresponds to experimental conditions.

One of the questions which arises in a qualitative study of the model is the existence of solutions of the corresponding system of equations. There are several papers in which the propagation problem for an exothermal reaction front is solved for a one-temperature model (cf. [2] and the bibliography given there).

For particular assumptions on the analogy between the concentration and temperature fields and the reaction rate function (see [3]), where the monotonicity of the solution as a function of the wave velocity was used in an essential way. In the present paper, the existence of the solution to the equations governing the process referred to above will be demonstrated. It turns out that the solution is not monotonic with respect to the wave velocity, and thus the proof of [3] does not apply. We give an asymptotic formula for the wave velocity which corresponds to the approximate solution of [1].

1. Statement of the Problem. As in [1], the steady-state equations for the propagation of combustion waves in an inert, porous medium for the filtration of a combustible gas mixture have the form

$$\begin{gathered} a_\Theta\, d^2\Theta/dx^2 + u d\Theta/dx + \alpha_\Theta(T-\Theta) = 0, \\ (v-u)dT/dx + \alpha_T(T-\Theta) = (Q/c_T)w(n,T), \\ (v-u)dn/dx = -w(n,T),\ u \neq v, \end{gathered} \tag{1.1}$$

where Θ and T are the temperatures of the solid structure and gas, respectively; n, relative mass concentration of the solute; v, flow velocity; u, wave velocity; $\alpha_\Theta = \alpha_0 S/(1-\varepsilon)c_\Theta\rho_\Theta$; $\alpha_T = \sigma\alpha_\Theta$; $\sigma = (1-\varepsilon)c_\Theta\rho_\Theta/(\varepsilon c_T\rho_T)$; α_0, heat-exchange coefficient; S, specific area; ε, porosity constant; c_Θ, ρ_Θ and c_T, ρ_T, specific heats and densities of the solid structure and gas,

Institute of Chemical Kinetics and Combustion, Siberian Branch, Academy of Sciences of the USSR. Novosibirsk. Translated from Zhurnal Prikladnoi Mekhaniki i Tekhnicheskoi Fiziki, No. 6, pp. 67-71, November-December, 1983. Original article submitted June 11, 1982.

 0021-8944/83/2406-0824$07.50